

This is the accepted manuscript made available via CHORUS. The article has been published as:

Spin-orbital liquid and quantum critical point in
 $\text{Y}_{1-x}\text{La}_x\text{TiO}_3$

Z. Y. Zhao, O. Khosravani, M. Lee, L. Balicas, X. F. Sun, J. G. Cheng, J. Brooks, H. D. Zhou,
and E. S. Choi

Phys. Rev. B **91**, 161106 — Published 21 April 2015

DOI: [10.1103/PhysRevB.91.161106](https://doi.org/10.1103/PhysRevB.91.161106)

Spin-orbital liquid and possible quantum critical point in $Y_{1-x}La_xTiO_3$

Z. Y. Zhao,¹ O. Khosravani,² M. Lee,² L. Balicas,³ X. F. Sun,^{4,5,6}

J. G. Cheng,⁷ J. Brooks,^{2,3} H. D. Zhou,^{1,3} and E. S. Choi³

¹*Department of Physics and Astronomy, University of Tennessee, Knoxville, Tennessee 37996-1200, USA*

²*Department of Physics, Florida State University, Tallahassee, Florida 32306-3016, USA*

³*National High Magnetic Field Laboratory, Florida State University, Tallahassee, Florida 32310-3706, USA*

⁴*Hefei National Laboratory for Physical Sciences at Microscale,*

University of Science and Technology of China, Hefei, Anhui 230026, People's Republic of China

⁵*Key Laboratory of Strongly-Coupled Quantum Matter Physics,*

Chinese Academy of Sciences, Hefei, Anhui 230026, People's Republic of China

⁶*Collaborative Innovation Center of Advanced Microstructures,*

Nanjing, Jiangsu 210093, People's Republic of China

⁷*Beijing National Laboratory for Condensed Matter Physics, and Institute of Physics,*

Chinese Academy of Sciences, Beijing 100190, People's Republic of China

The specific heat, the susceptibility under pressure, and the dielectric constant were measured for single crystals $Y_{1-x}La_xTiO_3$. The observed T^2 -dependent specific heat at low temperatures for $0.17 \leq x \leq 0.3$ samples shows a spin-orbital liquid state between the ferromagnetic/orbital ordering ($x < 0.17$) and antiferromagnetic/possible orbital liquid phase ($x > 0.3$). The non-monotonous pressure-dependence of T_C and the glassy behavior of the dielectric loss for $x = 0.23$ sample suggest that it is approaching a possible quantum critical point. All these exotic properties are resulted from the coupling between the strong spin and orbital fluctuations while approaching the phase boundary.

PACS numbers: 72.80.Ga, 75.30.Et, 75.40.-s, 71.70.Ej

Transition-metal oxides with one or two electrons in the triply degenerate t_{2g} orbit, such as perovskite $RTiO_3$,¹⁻⁴ RVO_3 (R : rare earth elements and Y)⁵⁻⁷ and spinel $MgTi_2O_4$,⁸⁻¹⁰ AV_2O_4 ($A = Cd, Mn, Fe, Zn, Mg,$ and Co),¹¹⁻¹³ have orbital degree of freedom and could exhibit complex electronic and magnetic properties. The observed phenomena, such as structural distortion, metal-insulator transition, and magnetic phase transition, are usually coupled to the orbital ordering of the transition metals.

For example in $RTiO_3$, with increasing ionic size of R^{3+} , the distortion of the $TiO_{6/2}$ octahedra decreases and the system switches from ferromagnetism (FM) in $YTiO_3$ ($T_C = 26$ K) to antiferromagnetism (AFM) in $LaTiO_3$ ($T_N = 140$ K).¹⁴ Moreover, for $YTiO_3$, there is an orbital ordering state (OO) below T_C .^{15,16} On the other hand, for $LaTiO_3$, the neutron scattering experiments showed an orbital disorder, or orbital liquid (OL) state below T_N .^{17,18} However, some other experiments such as thermal conductivity,¹⁹ anomalies of the lattice parameters,^{20,21} thermal expansion,²² and NMR²³ suggested an orbital ordering state in $LaTiO_3$. While the orbital ground state of $LaTiO_3$ is still on debate, the common believes are (i) the increased La-doping in $Y_{1-x}La_xTiO_3$ can continuously change the system from FM to AFM state²⁴⁻²⁶ and (ii) near the phase boundary, spin and orbital fluctuations are expected due to the competitions between the different ground states with different magnetic interactions. These fluctuations lead to exotic physical properties. For example, the theoretical studies predicted a quantum critical point (QCP) on the phase boundary for $Y_{1-x}La_xTiO_3$.¹⁵ The under-

standing of the role of the orbital fluctuations in the orbital ordered systems will advance the understanding of the role of orbital degree of freedom in the complex oxide systems mentioned above.

So far, experiments have shown that the FM to AFM phase transition occurs around $x = 0.3$ for $Y_{1-x}La_xTiO_3$.²⁴ The optical measurements further showed that there are orbital fluctuations in $x < 0.2$ samples.²⁷ However, two key questions related to the exotic behaviors near the phase boundary are still unclear: (i) How exactly does the FM/OO phase evolve to AFM/possible OL phase? (ii) Does a QCP really exist on the phase boundary and what are its properties? In this Rapid Communication, we measured the specific heat, the susceptibility under pressure, and the dielectric constant of single crystals $Y_{1-x}La_xTiO_3$ ($x = 0, 0.12, 0.17, 0.23,$ and 0.3) to explore these questions.

Single crystals of $Y_{1-x}La_xTiO_3$ were grown by using the floating zone technique.¹⁹ The oxygen stoichiometry of all samples were checked by thermogravimetric measurements. The obtained δ in all $Y_{1-x}La_xTiO_{3+\delta}$ is about 0.001. The powder x-ray diffraction measurements on the grinded crystals confirm the pure phase and the Laue back diffraction pattern confirms the quality of the crystals. The specific heat measurements were performed on a physical property measurement system (Quantum Design). Hydrostatic pressures up to $P = 8$ kbar were obtained in a Be-Cu cell from HMD, using Pb as an internal manometer. The susceptibility measurements were done in a DC superconducting quantum interference device (Quantum Design) with an applied magnetic field 500 Oe. The dielectric constant was mea-

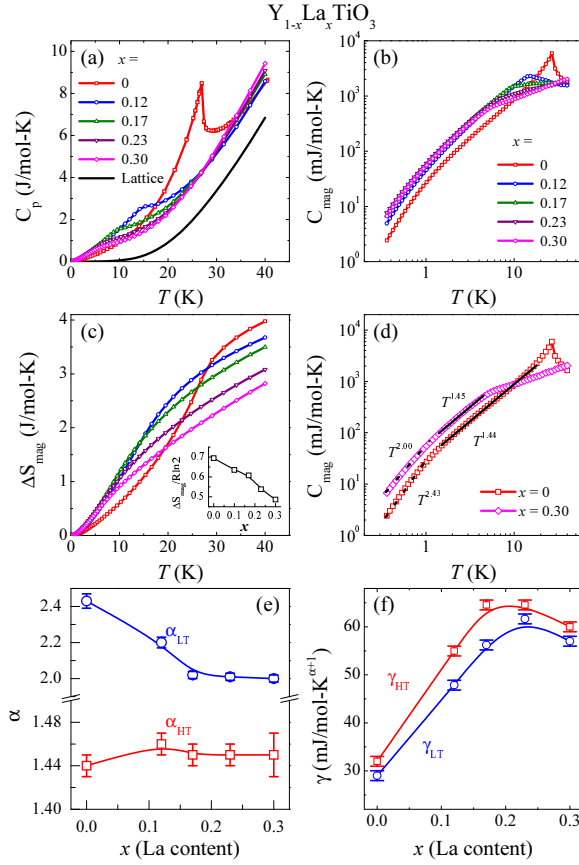


FIG. 1: (Color online) (a) Temperature dependencies of the specific heat (C_p) for $Y_{1-x}La_xTiO_3$ samples; here the lattice contribution is simulated by using the method described in Ref. 19. (b) The temperature dependencies of the magnetic specific heat (C_{mag}) for $Y_{1-x}La_xTiO_3$. (c) The variation in magnetic entropy ΔS_{mag} below 40 K. Insert: $\Delta S_{mag}/R\ln 2$ vs the La-content (x). (d) C_{mag} for $x = 0$ and 0.3 samples (open symbols); the solid and dash lines are the fits as described in the main text. The La-content (x) dependencies of the fitting parameters (e) α and (f) γ for C_{mag} .

sured with the techniques as reported in Ref. 28.

The specific heat C_p of $Y_{1-x}La_xTiO_3$ have been measured in zero field, as shown in Fig. 1(a). $YTiO_3$ shows a λ shape peak at $T_C = 26$ K, which is typical for a second order phase transition. This behavior is consistent with the reported data.²⁹ With increasing La-doping, the peak moves to lower temperatures and becomes broader. For $x = 0.12$ and 0.17 samples, the T_C is 15 K and 11.2 K respectively. For $x = 0.23$ and 0.3 samples, the peaks are so broad that it is difficult to define T_C from the specific heat data. The magnetic contribution of specific heat is shown in Fig. 1(b). The lattice contribution is simulated by using the method described in Ref. 19 and subtracted from the total C_p . The variation of magnetic entropy ΔS_{mag} below 40 K is calculated by integrating C_{mag}/T and is shown in Fig. 1(c). With increasing La-doping, ΔS_{mag} decreases from 4 J/mol-K for $YTiO_3$ to

2.5 J/mol-K for $Y_{0.7}La_{0.3}TiO_3$. These values correspond respectively, to 70% and 44% of $R\ln 2$ for an $S = 1/2$ system for Ti^{3+} ($3d^1$) ions, where R is the gas constant.

It is noteworthy that C_{mag} at low temperatures for $Y_{1-x}La_xTiO_3$ follows a γT^α behavior. As shown in Fig. 1(d), a linear fit of C_{mag} for $YTiO_3$ plotted in a log-log scale yields $\gamma_{HT} = 32$ mJ/mol-K^{2.44} and $\alpha_{HT} = 1.44$ for 1.5 K $< T < 18$ K and $\gamma_{LT} = 29$ mJ/mol-K^{3.43} and $\alpha_{LT} = 2.43$ for 0.35 K $< T < 1.3$ K. On the other hand, the fit of C_{mag} for $x = 0.3$ sample yields $\gamma_{HT} = 60$ mJ/mol-K^{2.45} and $\alpha_{HT} = 1.45$ for 1.5 K $< T < 4.5$ K and $\gamma_{LT} = 57$ mJ/mol-K^{3.0} and $\alpha_{LT} = 2.0$ for 0.35 K $< T < 1.1$ K. Figures 1(e)-(f) show the fitted results for all studied samples, and three notable features should be pointed out: (i) α_{HT} keeps a constant around 1.45 for all samples; (ii) α_{LT} is initially decreases with increasing x and then is almost the same as 2.0 for $x \geq 0.17$ samples; (iii) both γ_{HT} and γ_{LT} initially increases with increasing x and then keep at a similar value for $0.17 \leq x \leq 0.3$ samples.

The sharp peak from C_p and the recovered 70% of $R\ln 2$ magnetic entropy (more magnetic entropy could occur at T higher than 40 K²⁹) support the fact that $YTiO_3$ has a saturated FM order at $T_C = 26$ K. Below T_C , the fit of C_{mag} gives $\alpha = 1.44$ (near 1.5) with 1.5 K $< T < 18$ K and then 2.43 (near 2.5) with lower temperatures 0.35 K $< T < 1.3$ K; these exponents are characteristics for a ferromagnet with a quadratic magnon dispersion.³⁰ Meanwhile, $LaTiO_3$ has a G -type AFM order at $T_N = 140$ K with weak ferromagnetism. With increasing La-doping, the T_C of $Y_{1-x}La_xTiO_3$ decreases and eventually a FM-AFM phase transition occurs around $x = 0.3$. The decrease of the specific heat peak position and broadening of this peak with increasing x reported here are consistent with this fact. Moreover, due to the strong anisotropies of the magnetic couplings near the FM-AFM phase boundary, both T_C and T_N are expected to be suppressed while magnetic instabilities or strong spin fluctuations are expected to appear. The fact that ΔS_{mag} decreases with increasing x and is just 44% of $R\ln 2$ for $x = 0.3$ sample indicates that the sample is not fully ordered but has a short-range order nature, which should be resulted from the strong spin fluctuations while approaching the phase boundary.

Another noteworthy feature from our specific heat data is that for $0.17 \leq x \leq 0.3$ samples, the C_{mag} fit gives an α near 1.5 (consistent with the FM) above 1.5 K but an α near 2.0 below 1.5 K. This T^2 behavior certainly deviates from $T^{2.5}$ for the typical FM as shown by $YTiO_3$ at low temperatures. The theory on OL state in $LaTiO_3$ proposed a T -linear specific heat below T_N ,¹⁷ which also doesn't fit to the T^2 behavior observed here. Meanwhile, the theoretical studies on $Y_{1-x}La_xTiO_3$ have proposed that in the proximity area of the AFM/FM (OO/possible OL) phase boundary, the fluctuating part of the overall superexchange interactions dominates, which makes the separation of the spin and orbital degree of freedom might no longer be possible.¹⁵ The existence of the strong coupling between the spin and orbital fluctuations therefore

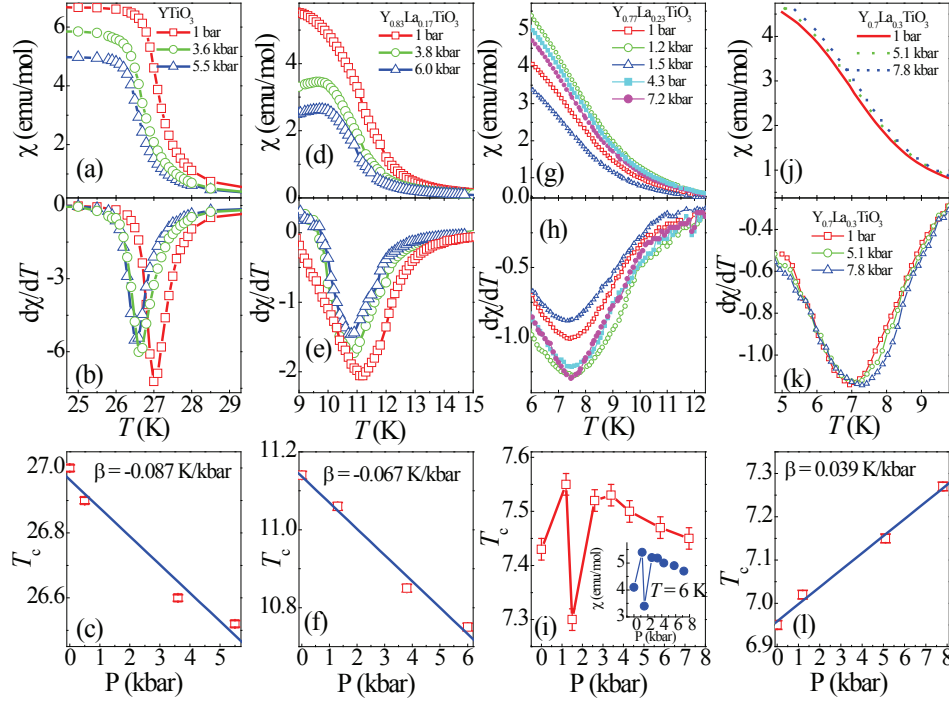


FIG. 2: (Color online) The magnetic susceptibility χ at different pressures, the $d\chi/dT$ vs T curves, and the pressure dependencies of T_C for $x = 0$ (a-c), 0.17 (d-f), 0.23 (g-i), and 0.3 (j-l), respectively. The solid lines in (c), (f) and (l) are linear fittings. Insert of (i): the pressure dependence of χ for $x = 0.23$ at 6 K.

can lead to a spin-orbital liquid (SOL) state, in which both spin and orbital show short-range ordered states. Actually this T^2 behavior of specific heat is the same as the recently studied SOL candidate LaSrVO_4 ³¹ and also very similar to several other studied SOL candidates LiNiO_2 ³² and FeSc_2S_4 ,³³ both of which show a $T^{2.5}$ behavior of specific heat at low temperatures. Therefore, the T^2 -dependent specific heat observed for $0.17 \leq x \leq 0.3$ samples supports that the orbital fluctuations begin to show their effects on the thermal dynamics below 1.5 K. The fact that the decrease of magnetic entropy and T^2 -dependence occur almost simultaneously for $0.17 \leq x \leq 0.3$ samples again confirms the strong coupling between spin and orbital fluctuations. Our results support that there is an intermediate phase, SOL state, for $0.17 \leq x \leq 0.3$, when $\text{Y}_{1-x}\text{La}_x\text{TiO}_3$ evolves from FM/OO to AFM/possible OL state.

Furthermore, the theoretical studies proposed that this strong quantum magnetic and orbital instability should lead to a QCP on the phase boundary.¹⁵ The next goal is to find evidences for the possible QCP. For YTiO_3 , the OO transition occurs simultaneously with the FM transition at T_C and is mainly due to the GdFeO_3 -type distortion of the $\text{TiO}_{6/2}$ octahedra. The magnitude of this distortion depends on the radius of the rare earth element in RTiO_3 . Therefore, this distortion, or the transition temperature, is not only sensitive to the chemical pressure such as the La-doping in YTiO_3 but also phys-

ical pressure applied on the sample. We therefore performed the susceptibility measurement under pressure P for $\text{Y}_{1-x}\text{La}_x\text{TiO}_3$, as shown in Fig. 2. Here, T_C for all samples is defined as the peak position of $d\chi/dT$.

For YTiO_3 (Figs. 2(a-b)), both T_C and $\chi(T)$ below T_C decrease with increasing P . The linear fit ($T_C \propto \beta P$) for the pressure dependence of T_C yields $\beta = -0.087$ K/kbar (Fig. 2(c)). $x = 0.17$ sample shows similar behavior as YTiO_3 with $\beta = -0.067$ K/kbar. For $x = 0.23$ sample, with increasing pressure, $T_C = 7.43$ K at ambient pressure increases to 7.55 K at 1 kbar first, then decreases to 7.3 K at 1.5 kbar, and increases again to 7.54 K at 3 kbar, and then decreases again to 7.45 K at 7 kbar. Therefore the total pressure dependence of T_C for $x = 0.23$ is non-monotonous within a small range around T_C (Figs. 2(g-i)). Separated measurements on $x = 0.23$ sample show repeatable and consistent results. The value of $\chi(T)$ at 6 K below T_C for $x = 0.23$ also shows similar non-monotonous P dependence, as shown in the insert to Fig. 2(i). For $x = 0.3$ (Figs. 2(j-l)), both T_C and $\chi(T)$ below T_C increase with increasing P . The linear fit of the pressure dependence of T_C yields $\beta = 0.039$ K/kbar.

The thermal expansion studies on YTiO_3 ²⁹ suggested that T_C increases with increasing pressure along a axis, but decreases when the pressure is along b or c axis. The reported hydrostatic pressure dependence of T_C for YTiO_3 then is around -0.06 K/kbar. This value is simi-

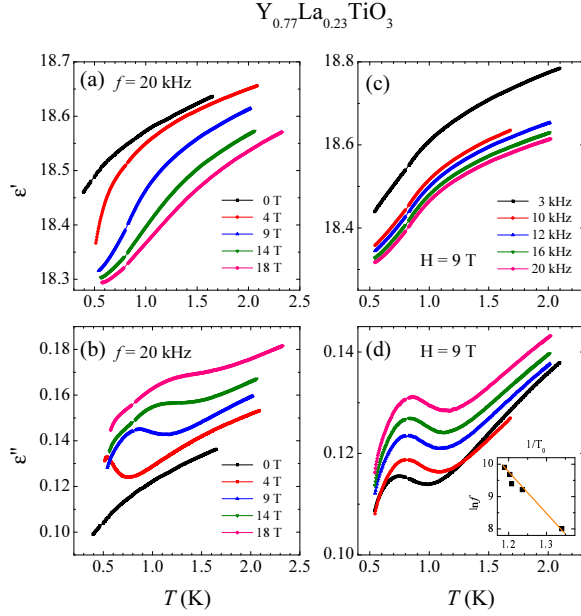


FIG. 3: (Color online) (a)-(b) Temperature dependencies of dielectric constant at different fields with constant frequency $f = 20$ kHz. (c)-(d) Temperature dependencies of dielectric constant under different frequencies at $H = 9$ T. Here, data in (a) and (c) is the real part ϵ' and data in (b) and (d) is the imaginary part ϵ'' . To clearly show the behavior of dielectric constant, an offset is made for (b)-(d) respectively. Insert: $\ln f$ vs the inverse dielectric loss peak temperature (T_0).

lar to our result here with $\beta = -0.087$ K/kbar. For $x = 0.17$ sample, $\chi(T)$ shows a similar but weaker pressure dependence ($\beta = -0.067$ K/kbar) as that of YTiO_3 . This shows that $x = 0.17$ sample should be on the same side of the phase diagram as YTiO_3 but with weaker distortion. For $x = 0.3$ sample, with increasing pressure, both $\chi(T)$ and T_C increase ($\beta = 0.039$ K/kbar), which are opposite to those for YTiO_3 . The pressure studies on LaTiO_3 also reported a positive pressure dependence of T_N with $\beta = 0.68$ K/kbar.³⁴ Therefore, the $x = 0.3$ sample is on the same side of the phase diagram as LaTiO_3 . By this meaning, the $x = 0.23$ sample has a good chance to approach the exact phase boundary. Indeed, for $x = 0.23$ sample, its pressure dependence of T_C and the value of $\chi(T)$ at 6 K show a non-monotonous behavior. This result supports that this sample is really approaching the phase boundary where strongly magnetic and orbital instability occurs. Since now with increasing pressure, the $x = 0.23$ sample can randomly select a ground state, either FM/OO or AFM/possible OL, which leads to the non-monotonous pressure dependence. This unique pressure dependence strongly suggests a possible QCP at $x = 0.23$ as the theory proposed.

Figure 3 shows the dielectric constant measured for $x = 0.23$ sample. While the dielectric constant (the real part, ϵ') and dielectric loss (the imaginary part ϵ'') show no obvious feature for phase transitions below 2 K at zero

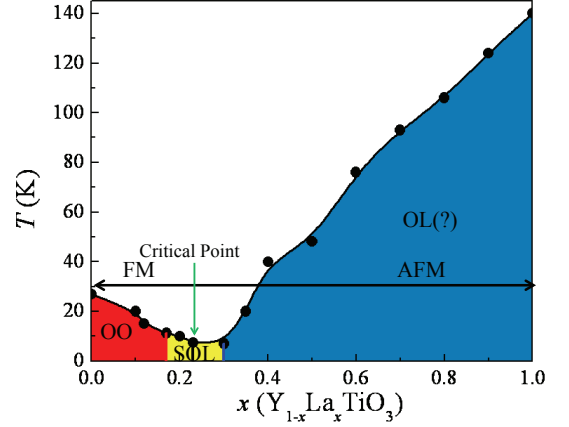


FIG. 4: (Color online) The schematic phase diagram for $\text{Y}_{1-x}\text{La}_x\text{TiO}_3$. The magnetic order temperatures (solid symbols) were obtained from the studies here and Ref. 24. The red regime represents the orbital order phase (OO), the yellow regime represents the spin-orbital liquid phase (SOL), and the blue regime represents the orbital liquid phase (OL). The critical point (QCP) is around $x = 0.23$. With $0 \leq x \leq 0.23$, the system is FM below T_C . With $0.23 < x \leq 1.0$, the system is AFM below T_N . The question mark for OL means that the OL state is still under debate.

field, the dielectric loss (Figs. 3(b,d)) begins to show a broad peak under applied fields. With increasing field, this peak moves to higher temperatures, typically around 1 ~ 1.5 K, and becomes more obvious. At $H = 9$ T, with increasing frequency this peak moves to higher temperatures (Fig. 3(d)).

The dielectric loss peak observed for $x = 0.23$ sample represents a typical feature of relaxational behavior for the glassy freezing of dipolar molecules, which actually is also observed for the orbital-glass state of FeCr_2S_4 .³⁵ Moreover, the dielectric loss observed for $x = 0.23$ sample is field dependent. At $H = 9$ T, the frequency dependence of the peak position (T_0) can be described by an Arrhenius law $f = f_0 \exp[-\Delta/(k_B T_0)]$. The linear fitting of the $\ln f \sim 1/T_0$ curve (Fig. 3(d) insert) yields an energy barrier $\Delta/k_B = 12$ K. This field dependent glassy behavior shows that the glassy state at low temperature for $x = 0.23$ is not only due to the orbital fluctuations but also related to the magnetism. This again supports that this sample is approaching the phase boundary with strong correlation of orbital and spin fluctuations in a SOL state.

In summary, we revisited the phase diagram (Fig. 4) for $\text{Y}_{1-x}\text{La}_x\text{TiO}_3$, and two important new features are observed: (i) within the $0.17 \leq x \leq 0.3$ regime, an intermediate phase, SOL phase, is located between the FM/OO and AFM/possible OL phases; (ii) a possible QCP is observed for $x = 0.23$ sample approaching the phase boundary. The exotic behaviors near this phase

boundary are dominated by the coupling between the strong spin and orbital fluctuations. Future studies are needed to further reveal the exact behaviors of the possible QCP at $x = 0.23$.

Acknowledgments

The NHMFL is supported by NSF-DMR-1157490 and the State of Florida. O.K. is supported by NHMFL-

UCGP funding. L.B. is also supported by DOE-BES through award DE-SC0002613. J.G.C. acknowledges the support from the National Science Foundation of China (Grant No. 11304371), the National Basic Research Program of China (Grant No. 2014CB921500), and the Chinese Academy of Sciences. X.F.S. acknowledges the support of the National Natural Science Foundation of China and the National Basic Research Program of China (Grant No. 2015CB921201). Z.Y.Z. and H.D.Z. thank the support of NSF-DMR-1350002.

-
- ¹ John B. Goodenough and J. S. Zhou, *J. Mater. Chem.*, **17**, 2394 (2007).
 - ² Y. Tokura and N. Nagaosa, *Science* **288**, 5465 (2000).
 - ³ G. Khaliullin, *Progress of Theoretical Physics Supplement* **160**, 155 (2005C).
 - ⁴ C. Ulrich, A. Gossling, M. Gruninger, M. Guennou, H. Roth, M. Cwik, T. Lorenz, G. Khaliullin, and B. Keimer, *Phys. Rev. Lett.* **97**, 157401 (2006).
 - ⁵ J. Q. Yan, J. S. Zhou, and John B. Goodenough, *Phys. Rev. Lett.* **93**, 235901 (2004).
 - ⁶ C. Ulrich, G. Khaliullin, J. Sirker, M. Reehuis, M. Ohl, S. Miyasaka, Y. Tokura, and B. Keimer, *Phys. Rev. Lett.* **91**, 257202 (2003).
 - ⁷ Y. Ren, T. T. M. Palstra, D. I. Khomskii, E. Pellegrin, A. A. Nugroho, A. A. Menovsky, and G. A. Sawatzky, *Nature* **396**, 441 (1998).
 - ⁸ M. Isobe and Y. Ueda, *J. Phys. Soc. Jpn.*, **71**, 1848 (2002).
 - ⁹ M. Schmidt, W. Ratcliff, P. G. Radaelli, K. Refson, N. M. Harries, and S. W. Cheong, *Phys. Rev. Lett.* **92**, 056402 (2004).
 - ¹⁰ H. D. Zhou and John B. Goodenough, *Phys. Rev. B* **72**, 045118 (2005).
 - ¹¹ S. H. Lee, H. Takagi, D. Louca, M. Matsuda, S. Ji, H. Ueda, Y. Ueda, T. Katsufuji, J. H. Chung, S. Park, S. W. Cheong, and C. Broholm, *J. Phys. Soc. Jpn.* **79**, 011004 (2010).
 - ¹² S. BlochBlanco-Canosa, F. Rivadulla, V. Pardo, D. Baldomir, J. S. Zhou, M. Garcia-Hernandez, M. A. Lopez-Quintela, J. Rivas, and John B. Goodenough, *Phys. Rev. Lett.* **99**, 187201 (2007).
 - ¹³ A. Kismarhardja, J. S. Brooks, A. Kiswandhi, K. Matsubayashi, R. Yamanaka, Y. Uwatoko, J. Whalen, T. Siegrist, and H. D. Zhou, *Phys. Rev. Lett.* **106**, 056602 (2011).
 - ¹⁴ K. Takubo, M. Shimuta, J. E. Kim, K. Kato, M. Takata, and T. Katsufuji, *Phys. Rev. B* **82**, 020401 (2010).
 - ¹⁵ G. Khaliullin and S. Okamoto, *Phys. Rev. Lett.* **89**, 167201 (2002).
 - ¹⁶ C. Ulrich, G. Khaliullin, S. Okamoto, M. Reehuis, A. Ivanov, H. He, Y. Taguchi, Y. Tokura, and B. Keimer, *Phys. Rev. Lett.* **89**, 167202 (2002).
 - ¹⁷ G. Khaliullin and S. Maekawa, *Phys. Rev. Lett.* **85**, 3950 (2000).
 - ¹⁸ B. Keimer, D. Casa, A. Ivanov, J. W. Lynn, M. v. Zimmermann, J. P. Hill, D. Gibbs, Y. Taguchi, and Y. Tokura, *Phys. Rev. Lett.* **85**, 3946 (2000).
 - ¹⁹ J. G. Cheng, Y. Sui, J. S. Zhou, John B. Goodenough, and W. H. Su, *Phys. Rev. Lett.* **101**, 087205 (2008).
 - ²⁰ R. Schmitz, Ora Entin-Wohlman, A. Aharony, A. Brooks Harris, and E. Muller-Hartmann, *Phys. Rev. B* **71**, 144412(2005).
 - ²¹ M. Cwik, T. Lorenz, J. Baier, R. Muller, G. Andre, F. Bouree, F. Lichtenberg, A. Freimuth, R. Schmitz, E. Muller-Hartmann, and M. Braden, *Phys. Rev. B* **68**, 060401 (2003).
 - ²² J. Hemberger, H. A. Krug von Nidda, V. Fritsch, J. Deisenhofer, S. Lobina, T. Rudolf, P. Lunkenheimer, F. Lichtenberg, A. Loidl, D. Bruns, and B. Buchner, *Phys. Rev. Lett.* **91**, 066403 (2003).
 - ²³ T. Kiyama and M. Itoh, *Phys. Rev. Lett.* **91**, 167202 (2003).
 - ²⁴ H. D. Zhou and John B. Goodenough, *Phys. Rev. B* **71**, 184431 (2005).
 - ²⁵ J. P. Goral, J. E. Greedan, and D. A. Maclean, *J. Solid State Chem.* **43**, 244 (1982).
 - ²⁶ Y. Okimoto, T. Katsufuji, Y. Okada, T. Arima, and Y. Tokura, *Phys. Rev. B* **51**, 9581 (2006).
 - ²⁷ L. Craco, S. Leoni, and E. Muller-Hartmann, *Phys. Rev. B* **74**, 155128 (2006).
 - ²⁸ J. Hwang, E. S. Choi, H. D. Zhou, J. Lu, and P. Schlottmann, *Phys. Rev. B* **85**, 024415 (2012).
 - ²⁹ W. Knafo, C. Meingast, A. V. Boris, P. Popovich, N. N. Kovaleva, P. Yordanov, A. Maljuk, R. K. Kremer, H. v. Lohneysen, and B. Keimer, *Phys. Rev. B* **79**, 054431 (2009).
 - ³⁰ A. I. Akhiezer, V. G. Baryakhtar, and S. V. Peletminskii, *Thermodynamics of ferromagnets and antiferromagnets. Spin Waves. Chap. 6.* North Holland, Amsterdam (1968).
 - ³¹ Z. L. Dun, V. O. Garlea, C. Yu, Y. Ren, E. S. Choi, H. M. Zhang, S. Dong, and H. D. Zhou, *Phys. Rev. B* **89**, 235131 (2014).
 - ³² Y. Kitaoka, T. Kobayashi, A. Koda, H. Wakabayashi, Y. Niino, H. Yamakage, S. Taguchi, K. Amaya, K. Yamaura, M. Takano, A. Hirano, and R. Kanno, *J. Phys. Soc. Jpn.* **67**, 3703 (1998).
 - ³³ V. Fritsch, J. Hemberger, N. Buttgen, E. W. Scheidt, H. A. K. von Nidda, A. Loidl, and V. Tsurkan, *Phys. Rev. Lett.* **92**, 116401 (2004).
 - ³⁴ Y. Okada, T. Arima, and Y. Tokura, *Phys. Rev. B* **48**, 9677 (1993).
 - ³⁵ R. Fichtl, V. Tsurkan, P. Lunkenheimer, J. Hemberger, V. Fritsch, H. A. Krug von Nidda, E. W. Scheidt, and A. Loidl, *Phys. Rev. Lett.* **94**, 027601 (2005).